Carbohydrate Polymers 81 (2010) 188–195

Contents lists available at ScienceDirect

Carbohydrate Polymers

journal homepage: www.elsevier.com/locate/carbpol

Degradation kinetics and molecular structure development of hydroxyethyl cellulose under the solid state mechanochemical treatment

Rong Chen, Chuanbin Yi, Hong Wu*, Shaoyun Guo**

The State Key Laboratory of Polymer Materials Engineering, Polymer Research Institute of Sichuan University, 24, South Section 1, Yihuan Road, Chengdu 610065, China

ARTICLE INFO

Article history:
Received 24 October 2009
Received in revised form 4 February 2010
Accepted 9 February 2010
Available online 4 March 2010

Keywords:
Hydroxyethyl cellulose
Mechanochemical treatment
Degradation
Kinetics
Non-solvent

ABSTRACT

The mechanochemical degradation behavior of hydroxyethyl cellulose (HEC) during vibratory ball milling and its induced morphological and structure development of HEC were studied through intrinsic viscosity measurement and scanning electron microscope (SEM), particle size analysis, wide-angle X-ray diffractometry (WAXD) and thermal gravimetry analysis (TG). A degradation kinetic model was proposed to evaluate the effects of ball-milling time on degradation rate of HEC with different initial molecular weights. The fragmentation mechanism is proposed based on the results of FTIR and ^{13}C NMR measurements. The experimental results indicated that the molecular weight decreased sharply with the increase of ball-milling time, charge ratio of steel ball/HEC and the rotational speed. Meanwhile, the fibriform morphology of original HEC was damaged observably and the crystallinity of HEC decreased sharply during the milling, which induced the decrease of the thermal stability.

1. Introduction

Hydroxyethyl cellulose (HEC), one of the most important cellulose derivatives, can be employed in extensive utilizations because of its wonderful water-solution properties and the chemical composition with a large amount of relatively easily accessible hydroxyl units that can be attached by a number of functional groups (Erkselius & Karlsson, 2005; Evertsson & Nilsson, 1999; Liedermann & Lapík, 2000; Sun, Sun, & Wei, 2007). Due to the β-D-glucose rings of the main chain of HEC, as well as the strong hydrogen bonds among the hydroxyl groups, these chemical modifications have mainly been realized through solution process, which would be usually expensive and relatively complex and its difficult to avoid byproducts (Eduardo & Ignacio, 2003; Li, Wang, & Huang, 2007; Videki, Klebert, & Pukanszky, 2007). Therefore, developing a new modification performed in solvent free condition for HEC is very profound.

Solid state mechanochemical reactions were widely applied to enhance the compatibility of polymer blends and composites, as well as to regulate and control the molecular weight and morphology of polymers in recent years (Huang, Lu, Li, & Tong, 2007). Here we focused on the process of vibratory ball milling, which was emphasized to be environmental benign and was undoubtedly one of the most suitable techniques for industrialization (Kim, Suzuki, Hagiwara, Yamaji, & Takai, 2001). The mechanochemical treatment of ball-milling operated successfully due to the strength of compression, shearing, attrition and impacting of balls that act onto materials. And because of the transformation from mechanical energy to chemical energy, several modes of fragmentation were found during the milling, such as abrasion, chipping and massive breakage (France, Bolay, & Belarouri, 2001). The ball-milling treatment was employed in the comprehensive fields and applications such as fine grinding of minerals and polymers, surface modification of materials and preparation of dry-blending systems (Hashimoto & Satoh, 2002; Molina-Boisseau & Bolay, 2000; Vertuccio, Gorrasi, Sorrentino, & Vittoria, 2009; Wongsaenmai & Tan, 2008). As a result of the prolonged milling action, when the transferred energy during the hit is high enough to overcome the activation barrier, a chemical bond is ruptured to produce a pair of free radicals, further chemical reactions may occur, due to which the mechanochemical modifications of poly(vinyl chloride) and polyethylene were investigated in our Laboratory (Guo, Wu, & Chen, 2003; Pi, Guo, & Ning, 2003; Pucciariello & Bonini, 2008; Xiong, Chen, & Guo, 2008). Takashi prepared a novel blend of cellulose and poly(ethylene glycol) by improving their compatibility through the formation of hydrogen bonds between the two composites during the milling (Endo, Kitagawa, & Zhang, 1999). Qiu prepared a cellulose-maleated polypropylene composite through the formation of ester bonds between them (Qiu, Endo, & Hirostu, 2004; Qiu, Endo, & Hiroysu, 2005). The structural alteration and recrystallization of cellulose were also studied by a ball-milling process (Ago, Endo, & Hirotsu, 2004; Ouajai & Shanks, 2006). From those reports, it can be demonstrated that solid

* Corresponding author. Tel.: +86 28 85466077; fax: +86 28 85466077.
** Corresponding author. Tel.: +86 28 85405135; fax: +86 28 85405135.
E-mail addresses: wh@scu.edu.cn (H. Wu), nic7702@scu.edu.cn (S. Guo).

0144-8617/$ – see front matter © 2010 Elsevier Ltd. All rights reserved.
doi:10.1016/j.carbpol.2010.02.012

state mechanochemistry is, indeed, a feasible approach to prepare biodegradable polymers with a wide variety of properties, which were hardly modified through traditional modification processing.

To the best of our knowledge, the researches of solid state mechanochemistry in polymer materials were mainly focused on the improvements of mechanical and chemical properties of materials and the degradation kinetics of polymers during the milling. The glass transition temperature of cellulosic material is usually far beyond ambient temperature, which causes an easier rupture of polymer chains and induces a wonderful milling effect. Meanwhile, because of the advantages of the ball milling as solvent free, low reaction temperature, low energy consumed and great efficiency, the ball-milling processing should be one of the most suitable methods used on the modification of cellulosic materials (Pucciariello & Bonini, 2008). In our previous work, the grafting copolymerization of hydroxyethyl cellulose with acrylic acid in ball milling was successfully achieved (Chen, Yi, Wu, & Guo, 2009). In this work, the degradation kinetics of HEC during the milling and effecting factors such as milling time, charge ratio of steel ball/HEC, rotational speed on mechanochemical degradation are studied. The development of morphological and crystalline structure of HEC and the thermal stability during the milling are discussed.

2. Experimental

2.1. Materials

Three kinds of commercial hydroxyethyl cellulose (HEC) powder was obtained from Xiangtai Corporation (Zhongxiang, China), with the molecular weights of 2.9×10^5, 1.9×10^5 and 1.0×10^5 g/mol (signed as HEC-1, HEC-2 and HEC-3, respectively), as determined by a viscosity method in deionized water at the temperature of 25 °C (Sato & Nalepa, 1978). The degree of substitution of HEC samples is 0.8–1.0, the molar substitution is 1.6–1.8.

2.2. Ball-milling degradation

The ball-milling degradation of HEC is conducted in a vibratory ball-milling machine, which is developed in our Lab. A steel cylindrical vessel, containing the milling medium (steel balls) and dry HEC, is instilled by a flow of cool water to fix the operating temperature at about 30 °C. The balls in the vessel are high-speed moved by the rotation of the steel bar. Then the HEC powder with different molecular weights were milled by the strength of compression, shearing, attrition and impacting of balls onto the HEC powder, with varied milling time, rotational speed and charge ratio.

2.3. Characterization

Viscosity measurements of HEC before and after milling in deionized water were carried out with an Ubbelodhe viscometer (Liangjing Co., Shanghai, China) at 25 ± 0.1 °C. The concentration range of HEC solutions are 0.9–1.1 g/100 ml, during which the η_r can be controlled in the range of 1.2–2.0. For each sample solution, the flow time was measured and the relative and specific viscosities were calculated according to

$$\eta_r = \frac{t}{t_o} \qquad \eta_{sp} = \eta_r - 1 \tag{1}$$

where t and t_o are the flow time for the HEC solution and the solvent, respectively.

The relationship between η_{sp} and $[\eta]$ can be described as

$$\frac{\eta_{sp}}{C} = \frac{[\eta]}{1 - k[\eta]C} = [\eta] + k[\eta]^2 C \tag{2}$$

If the $\eta_{sp} < 1$, Taylor series expansion of $\ln \eta_r$ can be expressed as

$$\ln \eta_r = \ln(1 + \eta_{sp}) = \eta_{sp} - \frac{\eta_{sp}^2}{2} + \frac{\eta_{sp}^3}{3} \cdots \tag{3}$$

From Eqs. (2) and (3), we can get the equation that

$$\frac{\ln \eta_r}{C} = [\eta] + \left(k - \frac{1}{2}\right)[\eta]^2 C + \left(\frac{1}{3} - k\right)[\eta]^3 C^2 + \cdots \tag{4}$$

When $k = 1/3$, an approximate equation can be obtained

$$\frac{\ln \eta_r}{C} = [\eta] + (k - 0.5)[\eta]^2 C \tag{5}$$

From Eqs. (1) and (4), intrinsic viscosity is (Taghizadeh & Asadpour, 2009).

$$[\eta] = \frac{[2(\eta_{sp} - \ln \eta_r)]^{1/2}}{C}. \tag{6}$$

where C is the solution concentration of HEC sample.

The viscosity-average molecular weight (M_η) was determined using the Mark–Houwink equation:

$$[\eta] = k[M_\eta]^\alpha \tag{7}$$

where α and k are the Mark–Houwink constants.

When the degree of substitution of HEC is 0.8–1.0, the molar substitution is 1.6–1.8 and the concentration of HEC is 1 g/100 ml in the solvent of deionized water, the $k = 4.70 \times 10^{-4}$, while $\alpha = 0.8$. So the viscosity-average molecular weight (M_η) was determined as (Sato & Nalepa, 1978):

$$[\eta] = 4.70 \times 10^{-4}[M_\eta]^{0.8} \tag{8}$$

The FTIR spectra of HEC and milled HEC were recorded for the purpose of characterizing the variation of the structure of HEC during the milling. The samples were measured on a Nicoet-560 spectrometer (Nicoet Co., USA) at a resolution of 2 cm^{-1} with accumulation of 32 scans in the spectral range of 4000–400 cm^{-1}.

The mechanism of fragmentation of polymer chains was further confirmed through ^{13}C NMR measurements by a DRX-400 Bruker spectrometer (Bruker Co., Germany). The HEC and the milled sample were dissolved overnight in D_2O at 40 °C.

The morphology of HEC powder with different milling times was observed under an Inspect F scanning electron microscope (Philips, Netherlands). A thin layer of Pd–Au alloy was coated on the specimen prior to measurement to prevent charging on the surface. SEM was operated at an accelerating voltage of 20 kV.

The average particle size and particle size distribution of HEC powder were measured by Mastersizer 2000 laser particle analyzer (Malvern Co., UK). The range of size analysis is 0.02–2000 μm. An appropriate amount of each sample was dispersed in isopropanol, stirred at a pumping speed of 2400 rpm. The specific surface area of HEC powder can be estimated simultaneously.

The crystalline structures of the samples were measured by a Philips X'pert Pro MPD wide-angle X-ray diffractometry (Philips, Netherlands), using Cu Kα X-rays with a voltage of 40 kV and a current of 20 mA. The samples were scanned with 2θ values ranged from 7° to 40° and the scanning speed was 2°/min.

The thermal stability of milled HEC samples was examined using a TGA Q500 analyzer (TA Instruments, USA). The measurements were taken in nitrogen flow at a heating rate of 10 °C/min with temperature range from 35 to 450 °C.

3. Results and discussion

3.1. Solid state mechanochemical degradation kinetics of HEC

One basic effect of the solid state mechanochemical degradation is shown in Fig. 1, in which the symbols illustrate the variation

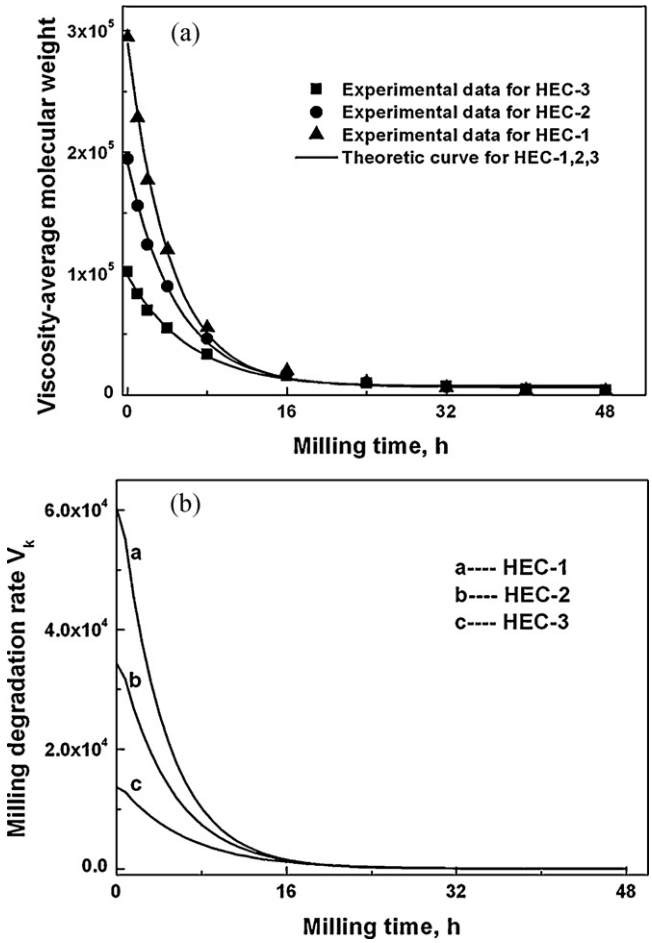

Fig. 1. Effect of milling time on viscosity-average molecular weight (a) and the degradation rate (b) of HEC with different initial molecular weight.

in viscosity-average molecular weight and degradation rate for HEC with different initial molecular weight. Clearly, the viscosity-average molecular weight of HEC strongly depends on the time of milling. In the first 8 h, HEC undergo great degradation, causing a significant decrease of viscosity-average molecular weight. After that, the viscosity-average molecular weight tends to a limiting value M_∞, below which no further degradation takes place. Considering the constant shortest polymer chains without rupture can be obtained under the constant mechanochemical effect for certain polymers, which is according to the limiting molecular weight M_∞, thus the M_∞ is constant and independent of the initial molecular weight of HEC.

Baramboim suggested that the kinetics of polymer degradation under stress could be expressed as Eq. (9), which is applied to describe the kinetics of solid state mechanochemical degradation in this work (Baramboim, 1964):

$$-\frac{d(M_t - M_\infty)/M_\infty}{dt} = k\left(\frac{M_t - M_\infty}{M_\infty}\right) \tag{9}$$

where M_∞ and M_t are the limiting molecular weight and average molecular weight at milling time t, respectively and k is the rate constant of degradation reaction.

By integrating and considering that at $t = 0$, $M_t = M_0$ (where M_0 is the initial molecular weight), Eq. (9) could be expressed as:

$$M_t = (M_0 - M_\infty)e^{-kt} + M_\infty \tag{10}$$

on designating the constant $M_0 - M_\infty = A$,

$$M_t = Ae^{-kt} + M_\infty \tag{11}$$

Table 1
The value of φ of HEC with different initial molecular weight.

Sample	HEC-1	HEC-2	HEC-3
φ	40.10	29.42	16.99

According to Eq. (11), the limiting molecular weight and the rate constant of degradation reaction could be obtained. The degradation rate at milling time t (v_t) could be expressed as the differential of Eq. (11):

$$v_t = -\frac{dM_t}{dt} = kAe^{-kt} \tag{12}$$

As demonstrated in Fig. 1(a), Eq. (11) describes the experimental data of M_η of HEC well. The equations of the theoretical curves are as follows:

$$M_{\text{HEC-1}} = 7.35 \times 10^3 + 28.26 \times 10^4 e^{-0.2346t}$$
$$(\text{HEC-1, related coefficient } R = 0.998) \tag{13}$$

$$M_{\text{HEC-2}} = 6.61 \times 10^3 + 18.41 \times 10^4 e^{-0.2021t}$$
$$(\text{HEC-2, related coefficient } R = 0.998) \tag{14}$$

$$M_{\text{HEC-3}} = 5.96 \times 10^3 + 9.21 \times 10^4 e^{-0.1581t}$$
$$(\text{HEC-3, related coefficient } R = 0.997) \tag{15}$$

According to Eqs. (13)–(15), HEC with different initial molecular weights have almost the same limiting molecular weight M_∞ when the milling conditions are unchanged.

Fig. 1(b) shows the relation of degradation rate v_t with milling time. The solid state mechanochemical degradation rate of HEC decreases greatly in first 8 h of ball milling and then tends to zero, indicating the end of the solid state mechanochemical degradation. It can be found that v_t of HEC-1 is larger than that of HEC-2 and HEC-3 is the smallest.

The mechanochemical degradation of HEC can be further studied by using a parameter, $\varphi = M_0/M_\infty$, which describes the extent of degradation. In other words, φ represents the average cleaving time of polymer chains. The data listed in Table 1 show that φ of HEC-1 is higher than HEC-2 and HEC-3, which is coincident with the discussion before.

3.2. *Effects of ball-milling conditions on the intrinsic viscosity ([η]) and viscosity-average molecular weight (M_η)*

From previous results on the effect of milling time on the M_η of HEC with different initial molecular weight, it is found that a rapid decrease in molecular weight is observed in all the three HEC samples under 8 h milling, in which the HEC-1 shows a greatest alteration. And then, the degradation of these samples all slows down in further prolonged milling time. Thus the HEC-1 sample was chosen with the milling time of 8 h to confirm the effect of ball-milling conditions on [η] and M_η of HEC.

The effects of ball-milling conditions on the intrinsic viscosity ([η]) and viscosity-average molecular weight (M_η) are shown in Fig. 2. Fig. 2(a) gives the effect of charge ratio of steel ball/HEC (charge ratio for short) on [η] and M_η of HEC samples, with the weight of HEC fixed to 300 g. When the charge ratio is lower, less degradation reaction of HEC happened because the energy transmitted to each particle is lower during the milling and the contacts between steel ball and reaction powder are less frequently, while

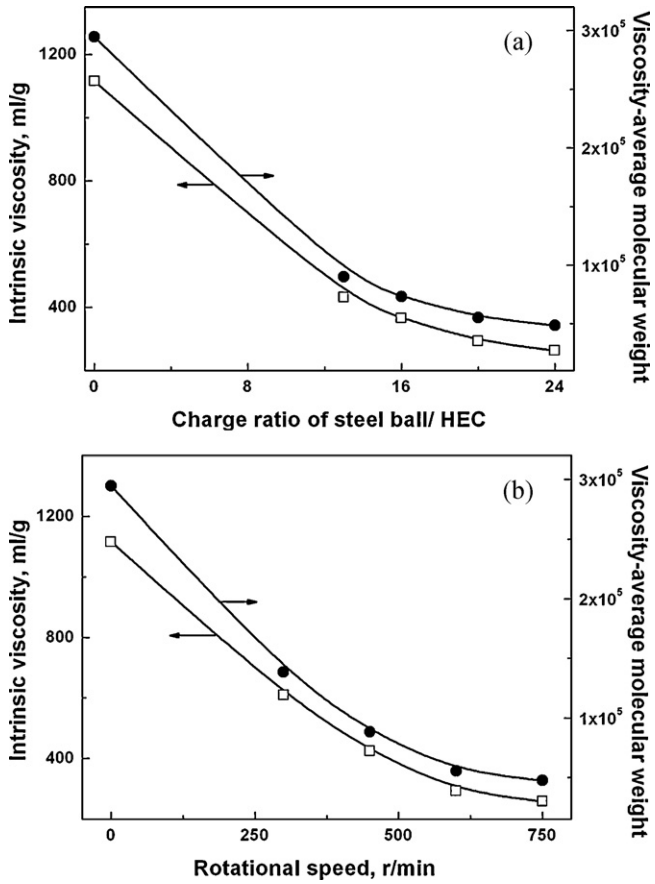

Fig. 2. Effect of charge ratio of steel ball/HEC (a) and rotational speed (b) on intrinsic viscosity (□) and viscosity-average molecular weight (●).

the contacts of polymer particles, which are inefficient to the degradation reaction, are increased (Molina-Boisseau & Bolay, 1999). With increasing the charge ratio from 13 to 20, more degradation reactions occur, leading to a smaller M_η of HEC. However, a further increase in charge ratio caused a slower decrease in M_η, which may be due to the fact that a high filling ratio would restrict the mobility of the steel ball and then result in a poor milling effect. On the other hand, when the charge ratio reached to 24, the rupture of HEC chains occurred more frequently, caused a faster approach of the M_η of HEC to the limiting value M_∞, which also slowed down the decrease of the M_η of HEC.

Fig. 2(b) shows that the [η] and M_η of HEC decreased with increasing the rotational speed. Under the lowest rotational speed of 300 r/min, the probability of the contacts between the steel balls and the polymers are lower, leading to a less effective milling of the polymeric particles. And the higher rotational speed caused higher shear force, which can result in the occurrence of more degradation reactions. When the rotational speed is beyond 600 r/min, a slower decrease in M_η can be observed, which may be due to the increase of the mobility of HEC fragment and the recombination reactions of HEC macroradicals.

3.3. Effects of ball milling on the molecular structure of HEC

As what were analyzed before, mechanochemical processes in open air were always accompanied by the introduction of polar groups onto polymer chains (Zhang, Liang, & Lu, 2007). And the FTIR analysis was performed to confirm whether new functional group was generated during the ball milling. The FTIR spectra of HEC before and after milling are shown in Fig. 3, which is

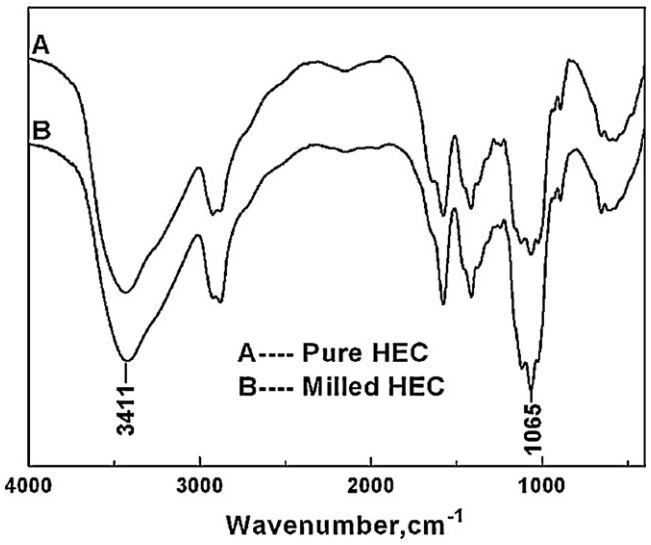

Fig. 3. FTIR analysis of HEC before (A) and after (B) milling.

consistent with the data earlier reported by Khutoryanskaya and Khutoryanskiy (Khutoryanskaya, Khutoryanskiy, & Pethrick, 2005). The absorbance at 3411 cm^{-1} corresponds to the O–H stretching vibration and the absorbance at 1067 cm^{-1} corresponds to the –C–O– stretching vibration. No new absorption peak appeared for HEC after milling, indicating that this process would not produce novel structure of HEC. The absorption peak at 1051 cm^{-1} corresponding to the C–O–C glycoside bond asymmetric stretching vibration shifted little after ball milling, which demonstrates that mechanochemical degradation of HEC can hardly occur at glucose rings. Indeed, the main degradation point should be at gly-

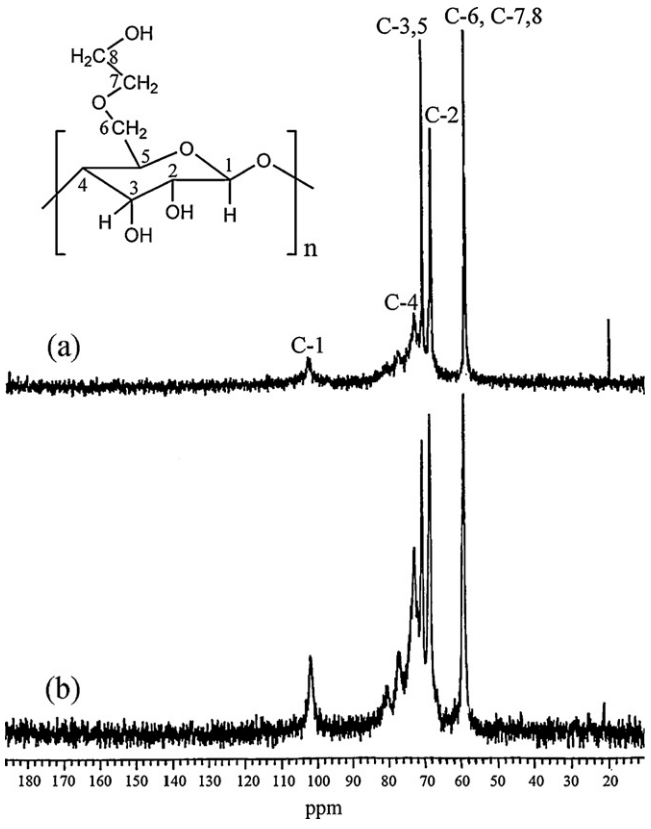

Fig. 4. ^{13}C NMR analysis of HEC before (A) and after (B) milling.

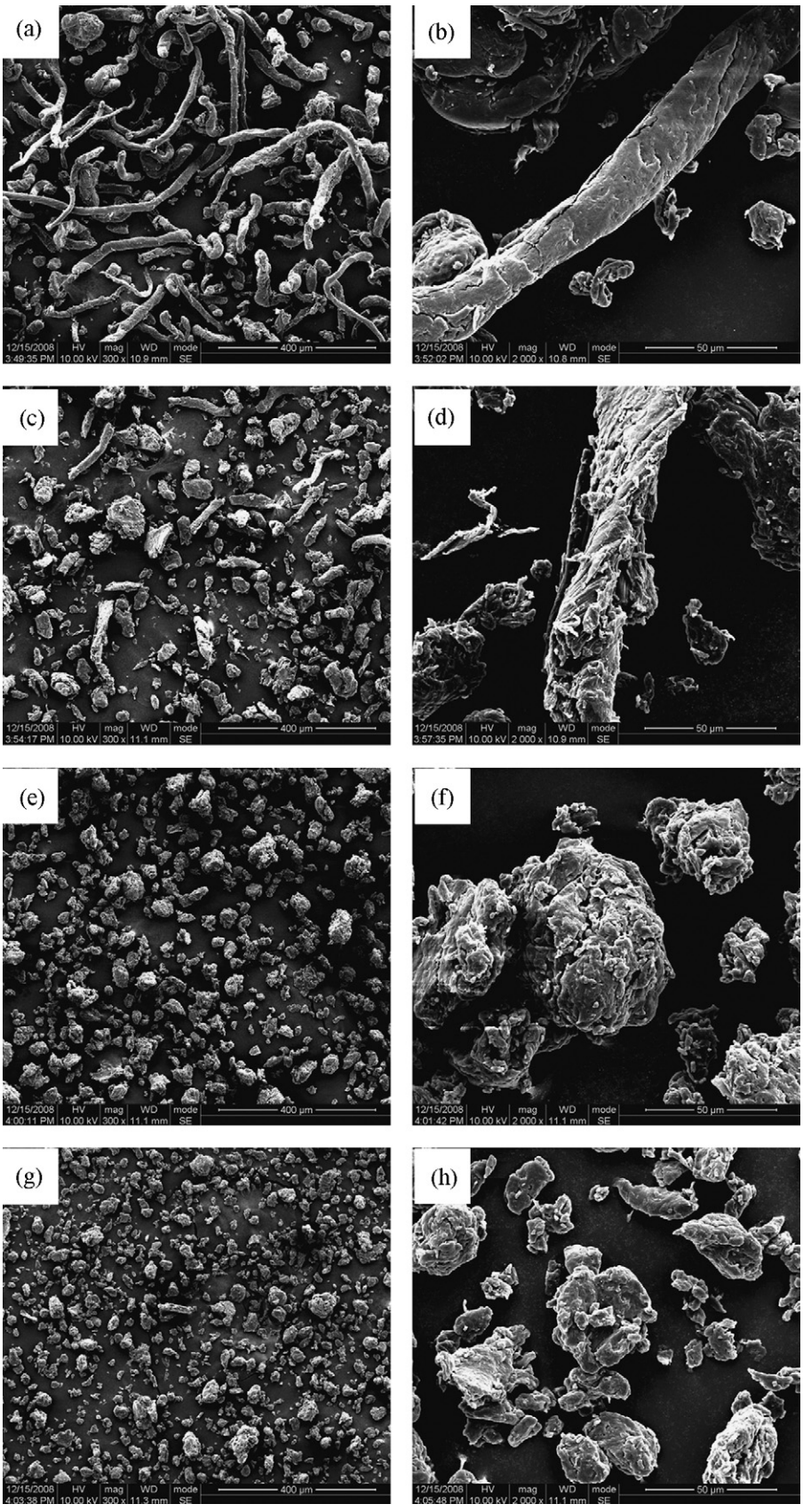

Fig. 5. SEM micrographs of pure HEC (a and b), milled HEC for 1 h (c and d), 4 h (e and f) and 8 h (g and h).

cosidic bonds, which can be also demonstrated by ^{13}C NMR analysis (Zhang, Lu, & Liang, 2007).

3.4. The degradation mechanism

The structure change of HEC was further confirmed from ^{13}C NMR analysis. As shown in Fig. 4, the peaks at range 60–110 ppm in the ^{13}C NMR spectrum of pure HEC are related to the ring carbons of HEC, which is consistent with related results in the literatures (Heinze & Liebert, 2001; Liu & Sun, 2007). There is no new peak appeared after ball milling, but the absorption intensity of each peak changed a little. Considering the tiny alteration of resonance signals exhibited by milled HEC, which is due to the sharply decrease in the viscosity of samples, it is reasonable that the intensity of each peak can be varied without introducing new functional groups. Meanwhile, the M_η of HEC decreased sharply during the milling, it can be well understood that the ball-milling processing caused a large amount of chain destruction of HEC, which mainly occurs in its skeleton structure instead of the ring-open reaction of the β-D-glucose rings of the main chain of HEC.

3.5. Effects of ball milling on morphological structure of HEC

The morphological structure of HEC after ball milling can be estimated according to the electron microscopic observation. SEM analysis of the surface morphology of HEC powder before and after milling is shown in Fig. 5. Fig. 5a and b is SEM micrographs of initial HEC powder, which consists of comparatively tangled fibres and bundles with smooth surface. Fig. 5c and d is SEM micrographs of HEC powder after 1 h milling, in which the HEC fibres began to lose their fibrillar structure and ground into small irregular particles, some with rough surface were also obtained. Fig. 5e and f is SEM micrographs of HEC powder after 4 h milling, the fibrous structure of HEC was completely destroyed and fine powder was produced due to the effects of steel-polymer impacting, shearing and pressing during the milling. As the milling time prolonged, to 8 h for example (Fig. 5g and h), the particle size of HEC became smaller and exhibited a more uniform and finer powder structure.

In order to further confirm the effects of solid state mechanochemistry to the morphological structure of HEC, the average particle size and particle size distribution of HEC powder were measured in Fig. 6. Fig. 6(a) shows the effects of ball milling on particle size and specific surface area of HEC. It is clearly found that the average size of HEC powder decreased sharply with the milling time, which is due to the pulverization of large particles and then decreased slightly after 4 h, with the reason that fine particles have a strong tendency to aggregate with each other in order to decrease the surface energy. The specific surface area increased with the milling time, indicating the separation and breakage of HEC fibres into small particles could produce more area at the cut edges.

The effect of ball milling on particle size distribution of HEC is shown in Fig. 6(b). The particle size of HEC powder moves to the smaller diameter with the increase of the milling time. Small fragments with size smaller than 100 μm were obtained, while the size distribution of the milled samples was relatively narrower than that of the original HEC. The particle size distributions was represented by the $D(v, 0.5)$ and the width of the size distribution was expressed quantificationally via the span, which were shown in Table 2. The span value was calculated as $[D(v, 0.9) - D(v, 0.1)]/D(v, 0.5)$, where the $D(v, p)$ is the equivalent diameter where p volume percentage of the particles has a smaller diameter and the remaining is coarser (Tang, Fletcher, Chan, & Raper, 2008). The $D(v, p)$ and the span values decreased with the prolonged milling time, which is consistent with the conclusions obtained before.

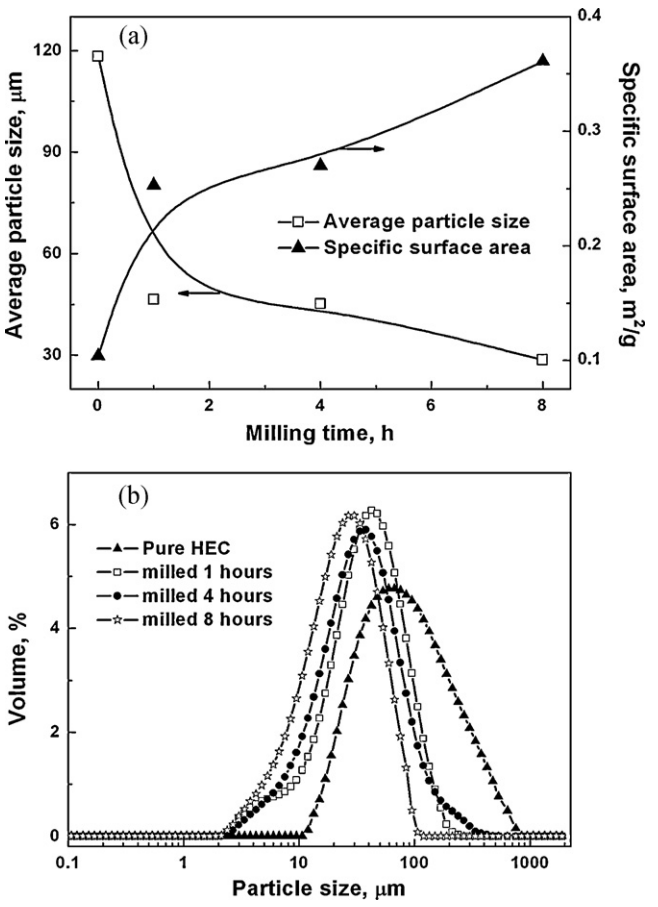

Fig. 6. Effect of milling on average particle size (□) and specific surface area (▲) (a) and particle size distribution (b) of HEC.

3.6. Effects of ball milling on crystalline structure of HEC

The WAXD diagrams of HEC and the milled HEC are shown in Fig. 7. The diffraction peak of the original HEC appears at $2\theta = 22^\circ$, which is characterized as cellulose I (Hadano & Onimura, 2003). In the initial stage of ball milling, the WAXD pattern of milled HEC still shows the identical peaks of cellulose I. However, these peaks become less intensive and wider, indicating the more amorphous characteristic. After 8 h milling, the milled HEC sample was in an almost amorphous state, indicating the destruction of crystalline region during the milling. These data demonstrated the obvious effect of ball milling on HEC powders, such as injecting, shearing and pressing. However, the WAXD pattern still shows the identical peaks of cellulose I, indicating that crystal type of HEC did not change after milling.

3.7. Effects of ball milling on the thermal stability of HEC

Fig. 8 gives the TG curves for the thermal stability of HEC before and after milling at a heating rate of 10 °C/min under a nitrogen atmosphere. The TG curve of original HEC has three distinct stages,

Table 2
Particle size of HEC powders during the ball milling.

Milling time, h	$D(v, 0.1)$ μm	$D(v, 0.5)$ μm	$D(v, 0.9)$ μm	Span
0	26.8	77.6	272.4	3.2
1	11.9	38.5	111.3	2.6
4	10.8	33.4	89.4	2.4
8	8.0	24.2	56.0	2.0

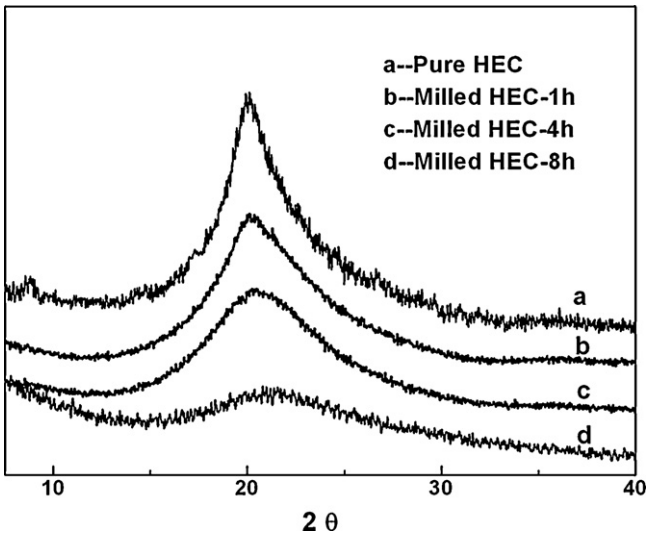

Fig. 7. WAXD analysis of cotton HEC before and after milling.

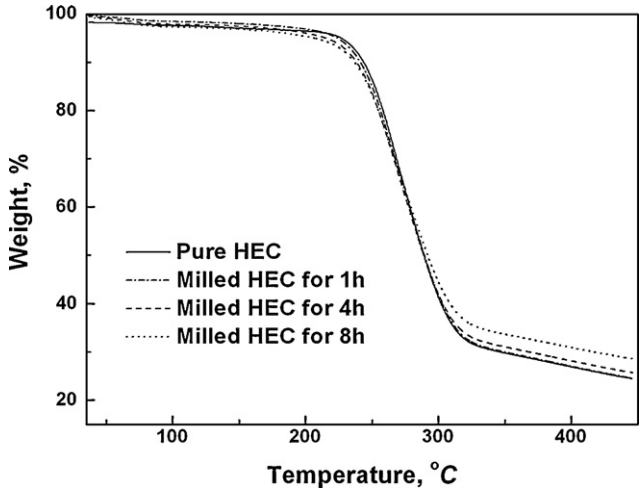

Fig. 8. TG curves of HEC before and after milling.

which is consistent with related result in the literature (Li, Huang, & Bai, 1999). The slight weight loss of HEC in the first stage is due to the physical desorption of water (intermolecular and intramolecular dehydration). In the second stage, the weight loss starts at 180 °C and continues to about 350 °C with a 67% weight loss, which is due to the removal of CO_2 or hydrocarbons. And the third stage starts due to the reactions of pyrolysis and carbonization. Table 3 shows the values of initial decomposition temperature (T_d) and the temperature corresponding to the maximum degradation rate (T_{dm}). It can be observed that in the second stage, the original HEC exhibits a better thermal stability than the milled one, which can be explained as the reduction of the particle size and the increase of HEC with lower molecular weight during the milling. The milled HEC exhibits a better thermal stability at the temperature beyond 300 °C, the reason of which is still unknown. It possibly indicated a higher degree of thermal resistance due to the micro-crosslinking structure which is caused by the dehydration of hydroxyl groups in the milled HEC samples.

Table 3
The T_d and T_{dm} of pure HEC and milled HEC for different times.

Sample	T_d (°C)	T_{dm} (°C)
Pure HEC	243	269
Milled HEC for 1 h	238	264
Milled HEC for 4 h	236	263
Milled HEC for 8 h	236	264

4. Conclusions

The molecular weight of HEC decreased sharply with the increase of milling time, charge ratio of steel ball/HEC and the rotational speed. The degradation kinetics is well described by Baramboim proposed kinetic equation. The molecular weight of HEC decreased with the increase of milling time and approached a limiting value, below which no further degradation took place.

HEC lost its fibriform morphology and irregular fine powder was obtained because of the effects of steel ball-polymer impacting, shearing and pressing during the milling. The average particle size decreased with the milling, while specific surface area increased gradually. The decrease in crystallinity and thermal stability of milled HEC was found because of the obvious effect of ball milling on HEC powder, such as injecting, shearing and pressing, while the crystal type of HEC did not change after milling.

Acknowledgements

The authors acknowledge the support of the Special Funds for Major State Basic Research Projects of China (2005CB623800) for this work.

References

Ago, M., Endo, T., & Hirotsu, T. (2004). Crystalline transformation of native cellulose from cellulose I to cellulose II polymorph by a ball-milling method with a specific amount of water. *Cellulose*, *11*, 163–167.
Baramboim, N. K. (1964). *Mechanochemistry of polymers*. Maclaren: Rubber and Plastic Research Association of Great Britain.
Chen, R., Yi, C. B., Wu, H., & Guo, S. Y. (2009). Solid state mechano-chemical grafting copolymerization of hydroxyethyl cellulose with acrylic acid. *Journal of Applied Polymer Science*, *112*, 3537–3542.
Eduardo, D. P., & Ignacio, M. V. (2003). Water-soluble polymer–metal ion interactions. *Progress in Polymer Science*, *28*, 173–208.
Endo, T., Kitagawa, R., & Zhang, F. R. (1999). Mechano-chemical preparation of novel cellulose–poly(ethylene glycol) composite. *Chemistry Letters*, 1155–1156.
Erkselius, S., & Karlsson, O. J. (2005). Free radical degradation of hydroxyethyl cellulose. *Carbohydrate Polymers*, *62*, 344–356.
Evertsson, H., & Nilsson, S. (1999). Microstructures formed in aqueous solutions of a hydrophobically modified nonionic cellulose derivative and sodium dodecyl sulfate: a fluorescence probe investigation. *Carbohydrate Polymers*, *40*, 293–298.
France, C., Bolay, N. L., & Belarouri, K. (2001). Particle morphology of ground gibbsite in different grinding environments. *International Journal of Mineral Processing*, *61*, 41–56.
Guo, S. Y., Wu, H., & Chen, G. S. (2003). Effect of high-energy vibro-milling of filler on the mechanical properties of filled high-density polyethylene. *Polymer Composites*, *24*, 456–463.
Hadano, S., & Onimura, K. (2003). Syntheses of chemical-modified cellulose obtained from waste pulp. *Journal of Applied Polymer Science*, *90*, 2059–2065.
Hashimoto, A., & Satoh, M. (2002). Fibrillation of aramid fiber using a vibrating ball mill and evaluation of the degree of fibrillation. *Journal of Matrials Science*, *37*, 4013–4017.
Heinze, T., & Liebert, T. (2001). Unconventional methods in cellulose functionalization. *Progress in Polymer Science*, *26*, 1689–1762.
Huang, Z. Q., Lu, J. P., Li, X. H., & Tong, Z. F. (2007). Effect of mechanical activation on physico-chemical properties and structure of cassava starch. *Carbohydrate Polymers*, *68*, 128–135.
Khutoryanskaya, O. V., Khutoryanskiy, V. V., & Pethrick, R. A. (2005). Characterisation of blends based on hydroxyethyl cellulose and maleic acid-alt-methyl vinyl ether. *Macromolecular Chemistry and Physics*, *206*, 1497–1510.
Kim, Y. J., Suzuki, T., Hagiwara, T., Yamaji, I., & Takai, R. (2001). Enthalpy relaxation and glass to rubber transition of amorphous potato starch formed by ball-milling. *Carbohydrate Polymers*, *46*, 1–6.
Li, X. G., Huang, M. R., & Bai, H. (1999). Thermal decomposition of cellulose ethers. *Journal of Applied Polymer Science*, *73*, 2927–2936.
Li, Z. X., Wang, L. G., & Huang, Y. (2007). Photoinduced graft copolymerization of polymer surfactants based on hydroxyethyl cellulose. *Journal of Photochemistry and Photobiology A: Chemistry*, *190*, 9–14.
Liedermann, K., & Lapík, L., Jr. (2000). Dielectric relaxation in hydroxyethyl cellulose. *Carbohydrate Polymers*, *42*, 369–374.

Liu, C. F., & Sun, R. C. (2007). Chemical modification of ultrasound-pretreated sugarcane bagasse with maleic anhydride. *Industrial Crops and Products*, *26*, 212–219.
Molina-Boisseau, S., & Bolay, L. N. (1999). Fine grinding of polymers in a vibrated bead mill. *Powder Technology*, *105*, 321–327.
Molina-Boisseau, S., & Bolay, N. L. (2000). Size reduction of polystyrene in a shaker bead mill-kinetic aspects. *Chemical Engineering Journal*, *79*, 31–39.
Ouajai, S., & Shanks, R. A. (2006). Solvent and enzyme induced recrystallization of mechanically degraded hemp cellulose. *Cellulose*, *13*, 31–44.
Pi, H., Guo, S. Y., & Ning, Y. (2003). Mechanochemical improvement of the flame-retardant and mechanical properties of zinc borate and zinc borate-aluminum trihydrate-filled poly(vinyl chloride). *Journal of Applied Polymer Science*, *89*, 753–762.
Pucciariello, R., & Bonini, C. (2008). Polymer blends of steam-explosion lignin and poly(ε-caprolactone) by high-energy ball milling. *Journal of Applied Polymer Science*, *109*, 309–313.
Qiu, W. L., Endo, T., & Hirostu, T. (2004). Interfacial interactions of a novel mechanochemical composite of cellulose with maleated polypropylene. *Journal of Applied Polymer Science*, *94*, 1326–1335.
Qiu, W. L., Endo, T., & Hiroysu, T. (2005). A novel technique for preparing of maleic anhydride grafted polyolefins. *European Polymer Journal*, *41*, 1979–1984.
Sato, T., & Nalepa, D. E. (1978). Shear degradation of cellulose derivatives. *Journal of Applied Polymer Science*, *22*, 865–867.
Sun, W. B., Sun, D. J., & Wei, Y. P. (2007). Oil-in-water emulsions stabilized by hydrophobically modified hydroxyethyl cellulose: adsorption and thickening effect. *Journal of Colloid and Interface Science*, *311*, 228–236.
Taghizadeh, M. T., & Asadpour, T. (2009). Effect of molecular weight on the ultrasonic degradation of poly(vinyl-pyrrolidone). *Ultrasonic Sonochemistry*, *16*, 280–286.
Tang, P., Fletcher, D. F., Chan, H. K., & Raper, J. A. (2008). Simple and cost-effective powder disperser for aerosol particle size measurement. *Powder Technology*, *187*, 27–36.
Vertuccio, L., Gorrasi, G., Sorrentino, A., & Vittoria, V. (2009). Nano clay reinforced PCL/starch blends obtained by high energy ball milling. *Carbohydrate Polymers*, *75*, 172–179.
Videki, B., Klebert, S., & Pukanszky, B. (2007). External and internal plasticization of cellulose acetate with caprolactone: structure and properties. *Journal of Polymer Science: Part B: Polymer Physics*, *45*, 873–883.
Wongsaenmai, S., & Tan, X. L. (2008). Dielectric and ferroelectric properties of fine grains $Pb(In1/2Nb1/2)O_3$-$PbTiO_3$ ceramics. *Journal of Alloys and Compound*, *454*, 331–339.
Xiong, Y., Chen, G. S., & Guo, S. Y. (2008). Solid mechanochemical preparation of core–shell SiO_2 particles and their improvement on the mechanical properties of PVC composites. *Journal of Polymer Science: Part B: Polymer Physics*, *46*, 938–948.
Zhang, W., Liang, M., & Lu, C. H. (2007). Morphological and structural development of hardwood cellulose during mechanochemical pretreatment in solid state through pan-milling. *Cellulose*, *14*, 447–456.
Zhang, X. X., Lu, C. H., & Liang, M. (2007). Preparation of rubber composites from ground tire rubber reinforced with waste tire fiber through mechanical milling. *Journal of Applied Polymer Science*, *103*, 4087–4094.